MECHANIKA TEORETYCZNA
I STOSOWANA
Journal of Theoretical
and Applied Mechanics
3, 31, 1993

NEW TRENDS IN OPTICAL METHODS FOR EXPERIMENTAL MECHANICS. Part I: MOIRE AND GRATING PROJECTION TECHNIQUES FOR SHAPE AND DEFORMATION MEASUREMENT

MAŁGORZATA KUJAWIŃSKA

KRZYSZTOF PATORSKI

Faculty of Fine Mechanics

Warsaw University of Technology

The influence of dynamic development in the field of personal computers and video techniques on optical methods used in the experimental mechanics is described. New methods of computer aided processing of the information encoded in the interferogram/moiregram patterns with special emphasis put on so-called phase methods are presented. The benefits of various modifications of the phase-stepping method are emphasized and illustrated by exemplary experimental results in the field of moire and grating projection topography used for the shape and deformation studies. The description of the equipment developed and sensitivity considerations are included.

1. Introduction

During the last thirty years new experimental techniques such as holographic and speckle interferometry, grating interferometry, wide range of moire techniques, optical heterodyning and modal analysis have emerged as the practical tool in the expanding field of experimental mechanics. The appearance of new materials and new disciplines, such as composite and smart materials and fracture mechanics have resulted in the introduction of traditional experimental techniques into new fields. These new developments, together with the dynamic uses of on/off-line computers for rapid data processing as well as a combined use of the experimental and the numerical techniques have significantly broadened the possibilities of experimental mechanics.

Herein we will focus on the development of optical techniques which are characterized by

- simultaneous providing with the whole field information

- noncontact and nondestructive measurement
- wide range of measurement sensitivity depending on the method being chosen (from nm to cm)
- high accuracy and measurement speed following from the computer aided processing of the experimental data.

The common feature of the optical methods considered, Fig.1, is coding the information required in the fringe pattern (interferogram)[1] in order to have the pattern analyzed accurately and rapidly and to present the results in the required numerical or graphical form.

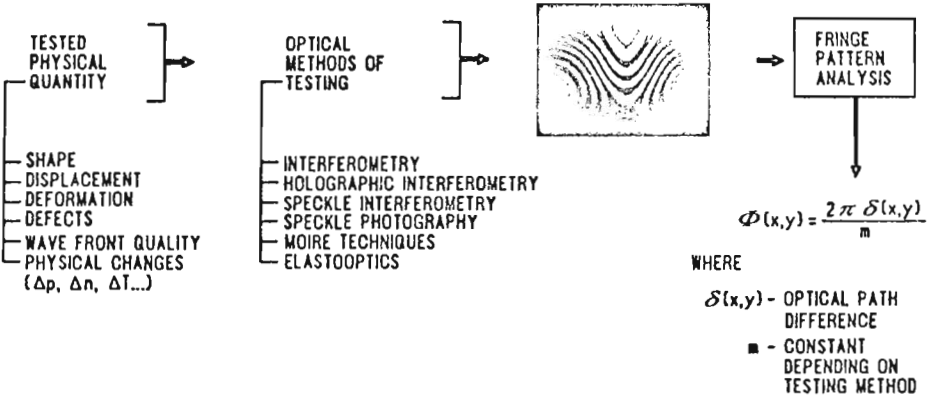

Fig. 1. Scheme of the analysis of various physical quantities by optical techniques

In the first Section advances of the automatic fringe pattern analysis methods and the description of an expert fringe pattern analysis system will be given. Next the principles, the newest concepts and instrumental developments of the selected optical techniques which implement the automatic analysis system will be presented. First the moire and grating projection techniques for shape and deformation measurement will be described. They represent a very powerful tool for laboratory and industrial tests when the sensitivity of the order of a few tenths of a millimeter or higher is required. The absolute or relative shape and out-of-plane displacements are obtained in after a few seconds only. In the next paper the technique of grating interferometry for submicron in-plane displacement measurement

[1]For brevity the term interferogram and fringe pattern will be used equivalently to describe the fringe-like patterns which are generated by the variety of optical systems, whether or not such patterns are generated by interferometric means. Broadening of the definition of interference is justified in the context of the work, since the mathematical descriptions and the image analysis procedures are essentially unaffected by the mechanism of fringe generation.

expanding recently will be presented. Due to its high resolution, wide strain range, excellent fringe contrast and relative ease for automation, it is especially suitable for material studies in both the macro and micro regions. The composite materials seem to benefit the most from the continuous development of the method.

2. Automatic fringe pattern analysis methods

2.1. Introduction

For long time the most difficult problem in fringe pattern analysis was getting the data from an interferogram without losing the inherent accuracy contained in it. In the sixties techniques using optical comparators, Dyson (1963), and photoelectric densitometers, Jones and Kakadia (1968), were developed for measuring the position of fringe centers, which were sent to a computer for analysis. These devices allowed a substantial improvement in the accuracy, but the overall process remained essentially manual and, by modern standards, extremely slow.

In the seventies faster techniques, using graphic tablets, video systems connected to computers, were developed for finding the fringes centers, Augustyn (1979). In the eighties digital processing systems became widely available, Robinson (1983). In most digital image processing systems, an image is detected by a television or CCD (couple charged device) cameras and television signal is fed into a "frame store". The frame store consists of a high speed analog-to-digital converter and electronic memory of a sufficient capacity. The use of image processing system influences the development of a great number of fringe pattern analysis methods.

Let us consider the general equation of fringe pattern

$$I(x,y) = a(x,y) + b(x,y)\cos\Phi(x,y) \tag{2.1}$$

In the process of fringe pattern analysis, the only measurable quantity is intensity $I(x,y)$. The unknown phase[2] $\Phi(x,y)$ should be extracted from Eq (2.1), although it is screened by two other functions: the background intensity $a(x,y)$ and the local contrast $b(x,y)$, Born and Wolf (1964). The intensity depends periodically on the phase to be measured, which causes two additional problems for the evaluation

– due to periodicity the phase is only determined mod 2π

[2]The term "phase" is used for the information on any principal quantity which is coded in the localization of the fringes in an interferogram. The process of fringe pattern analysis may be defined as the phase retrieving from an interferogram.

– due to the even character of the cosine function, that is $\cos\Phi = \cos(-\Phi)$, the sign of Φ cannot be extracted from a single measurement of $I(x,y)$ without an a priori knowledge.

Because of the above features of a fringe pattern, the proper acquisition and data processing system is not usually sufficient to generate an appropriate data base to enable a computer to perform an analysis of an interferogram. A single fringe pattern does not usually contain enough information to retrieve uniquely the phase coded. Two main approaches to solve the ambiguity of the problem are reported, Schwider (1990). The first one is the intensity based approach in which the fringe peaks are detected and the fringe orders are determined on the basis of the "a priori" knowledge. The second applies various concepts of phase-measuring methods including: temporal (heterodyne, phase-shifting, phase-locking) and spatial (Fourier transform, spatial synchronous detection, spatial phase-shifting) methods, respectively. Figure 2 shows the main techniques of automatic fringe pattern analysis. The phase measuring methods require, at one hand, various modifications of the optical or the electronic system generating the fringe pattern, but on the other hand give several advantages over the intensity method. These include the reduced sensitivity to the background and contrast variations in the fringe pattern, automatic sign detection and reduced or eliminated operator interaction.

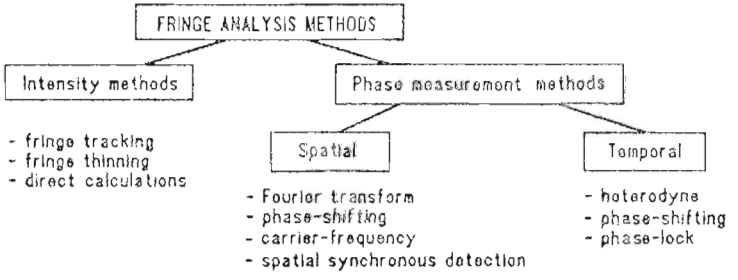

Fig. 2. Main fringe pattern analysis methods

Additionally the techniques for determining the phase from interferograms can be split into two categories: electronic (heterodyne, phase-lock, spatial synchronous detection) and analytical (intensity methods, Fourier transform and all variations of phase shifting techniques). To retrieve the phase electronically, hardware such as zero-crossing detectors, phase-lock loops and up-down counters are used to monitor interferogram intensity data as the phase is modulated. For analytical techniques, intensity data are recorded while the phase is temporally or spatially modulated, sent to computer and then used to compute the phase. There is no need for a scanning detector or using a large amount of redundant circuits. With the advent of powerful desk top computers and solid state detector arrays, the ana-

Table 1. Comparison of the analytical automatic fringe pattern analysis methods

	number of fringe pattern per frame	real time method	inherent image enhancement	inherent phase interpolation	automatic phase sign detection	automatic domain detection	achievable accuracy	experimental requirements	detector resolution requirements	complexity of processing	dynamic event analysis	comercial systems
intensity methods	1/1	NO	NO	NO	NO	NO	LOW	LOW	R_0 [1]	MEDIUM	NO	**
	2/2	NO	NO	NO	PARTLY	YES	LOW	LOW	R_0	MEDIUM	PARTLY	*
phase shifting • temporal	MIN 3/3	PARTLY	YES	YES	YES	YES	HIGH	HIGH	R_0	LOW	NO	****
• spatial	3/1	YES	PARTLY	YES	YES	YES	LOW	MEDIUM	$3R_0$	LOW	YES	
• carrier frequency	1/1	YES	PARTLY	YES	YES	YES	HIGH	LOW	MIN $2R_0$	LOW	YES	***
Fourier transform method	1/1	PARTLY	YES	YES	PARTLY	PARTLY	HIGH	LOW	MIN $2R_0$	HIGH	YES	*
	2/2	PARTLY	YES	YES	YES	YES	HIGH	MEDIUM	R_0	HARD-WARE	NO	*

[1] R_0 is the detector resolution required for the fringe pattern detection

lytical techniques have provided the most remarkable innovations in this field in the last years, Schwider (1990), Takeda (1990). The phase measurement methods of fringe pattern analysis, but intensity based methods, dominate in the research and commercially available systems. The most important features of analytical fringe pattern analysis methods are compared in Table I to facilitate the choice of the appropriate technique. The number of stars "*" indicate the popularity of the method in the commercially available systems. The letter "s" marks the methods applied in the multipurpose AFPA system designed at the Optical Engineering Division, the Warsaw University of Technology and presented below.

2.2. Architecture of the AFPA system

In general each method of a fringe pattern analysis includes three basic stages

1. Photoelectric detection of a fringe pattern.
2. Calculation of the phase.
3. Solutions of the modulo 2π and the sign problem.

These procedures are followed by the application oriented software which converts the phase information into the physical quantities required, e.g., shape, deformation, displacement, strain and many other merit functions or figures of merit.

The multipurpose system relies on two basic methods: Fourier transform, FT, Takeda (1990) and phase shifting, PS, Creath (1988). The last includes several versions: temporal PS (TPS), spatial (SPS) and carrier-frequency (SCPS) phase shifting method. There are two main differences between the methods considered. The first one shows up in the representation of the fringe pattern(s) recorded (stage 1) when compared with Eq (2.1). These include

— for the Fourier transform method-adding a spatial carrier frequency f_0

$$I(x,y) = a(x,y) + b(x,y)\cos[\Phi(x,y) + 2\pi f_0 x] \tag{2.2}$$

— for the temporal and spatial phase shifting methods-considering $n > 3$ fringe patterns with the known phase shifts $\delta_i = \frac{2\pi}{n} i$

$$I_i(x,y) = a(x,y) + b(x,y)\cos[\Phi(x,y) + \delta_i] \tag{2.3}$$

— for the spatial-carrier phase shifting method-introducing the known carrier frequency $f_0 = N/4$, where N is the sampling frequency of the detector used

$$I_i(x,y) = a(x,y) + b(x,y)\cos\left[\Phi(x,y) + 2\pi f_0\left(x + \frac{i}{4} f_0\right)\right] \tag{2.4}$$

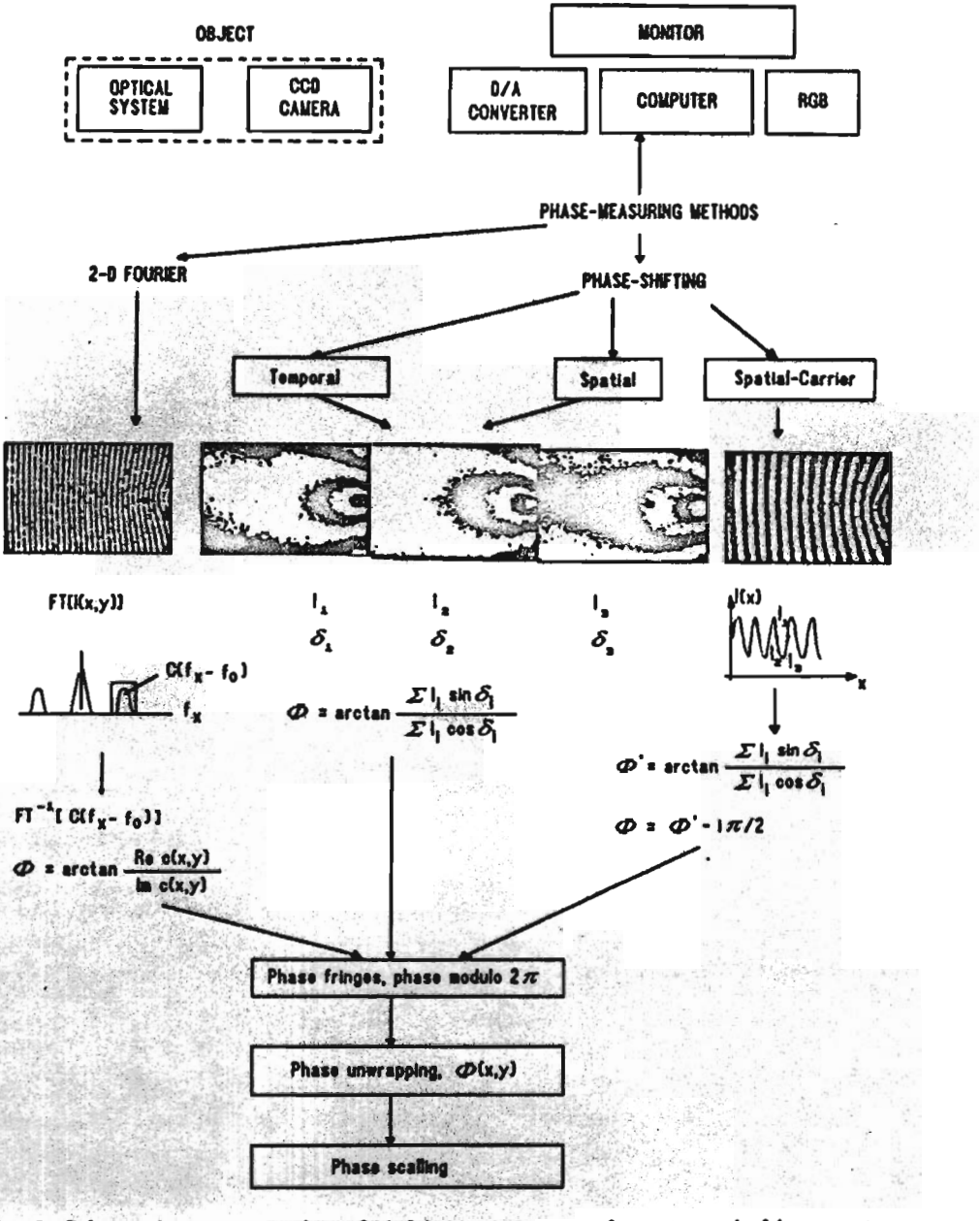

Fig. 3. Schematic representation of multipurpose system for automatic fringe pattern analysis

The second main difference appears at the stage of calculating the phase modulo 2π (Fig.3).

The Fourier Transform method is a global operation basing on separating the phase function on the spatial frequency plane, Takeda (1990). It is more complex in view of calculations, more difficult to have it totally automated, but it requires only a single fringe pattern and is not sensitive to nonlinear detection and background variations. However, as it was shown by Kujawińska and Wójciak (1991), the phase retrieved by FTM suffers from big errors at the edge of the fringe pattern domain. It restricts the applications of this method to several experimental mechanics problems.

The phase shifting techniques rely on operations performed separately for each point of the object. The principle of PS rests on setting a file of phase shift values and fitting a cosine function to the corresponding set of N intensity values at a single point. The temporal phase shifting TPS methods are defined as ones which combine three or more intensity measurements from a time series of images or points to provide a direct measurement of the phase distributions of fringe pattern. The system gives the choice of 3, 4 or 5 images algorithms, which are sensitive to different types of experimental errors, Creath (1988).

In spatial phase-shifting methods (SPS) all information necessary to reduce the fringe pattern to a phase map is recorded simultaneously. The information is retrieved from at least three separated in space phase-shifted fringe patterns, Kujawińska and Wójciak (1991).

In spatial-carrier phase-shifting method the simplicity of calculations due to the phase-shifting is brought together with a single interferogram analysis connected with the Fourier transform method. The main requirement here is introducing the proper carrier frequency into the fringe pattern, Kujawińska and Wójciak (1991). The operator may choose the three or five points algorithm in order to minimize the errors of the retrieved phase.

The system within the given method enables using various filters and unwrapping procedures an addition or subtraction of theoretical or experimental functions (plane, sphere and error functions).

The further stages: phase unwrapping, scaling of the results and calculating the physical quantities required are common for all phase measuring methods.

The errors obtained depend on errors of the particular method applied, the features of a fringe pattern (noise, the variations in background and contrasts functions) and the stability of the experimental arrangement. The FTM and SCPS methods tend to smooth (lose some information) within the area of larger gradients of the phase function. The SCPS method is the most sensitive to the noise in the interferogram. The results may be improved by the filtering process but it may cause further lost of the dynamic range of the phase function retrieved. The TPS method is the most accurate, however the conditions of the constant phase steps

and temporal stability of the system have to be fulfilled. Otherwise the phase suffers from the sinusoidal error with the frequency double to the fringe pattern frequency.

Figure 3 shows the schematic representation of the multipurpose system which was successfully used for the shape measurement using projection moire and fringe projection systems as well as for the in-plane displacement measurement by grating interferometry, as will be shown in the next sections. However the same system may be used for the automatic fringe pattern analysis of the results obtained by other optical methods of testing.

The multipurpose system presented enables the quantitative, automatic analysis of fringe patterns obtained from a great variety of optical methods applied for both static and dynamic events. The modular software structure gives the possibility of using common blocks, together with numerous paths to get the results in most efficient way.

3. Moire topography

The moire effect is a powerful tool for displaying and measuring in-plane and out-of-plane occurrences in the objects under load (Theocaris, 1969; Durelli and Parks, 1970; Chiang, 1979; Sciammarella, 1982; Patorski, 1993). In this Section we will focus on the computer aided shape and out-of-plane displacement measurements only since especially these applications can be automated and the investigations can be done in quasi-real time.

"Moire Topography" is done by three main techniques

- reflection moire
- shadow moire
- projection moire.

The first is used for objects which give specular reflection (basic limitation of the method) and is mainly applied to the determination of the shape of the surface in flexure of thin plates and shells. The other two methods are used for objects which reflect light diffusely. When compared with the shadow moire technique the projection method has the advantage that objects of considerable dimension can be contoured and the resulting fringe pattern is much easier to process automatically. Therefore in the following we will focus our interest on the projection moire method and its modified version with the grating or fringe pattern projected without using the detection grating for generating the moire fringes.

An experimental system for projection moire topography is shown schematically in Fig.4.

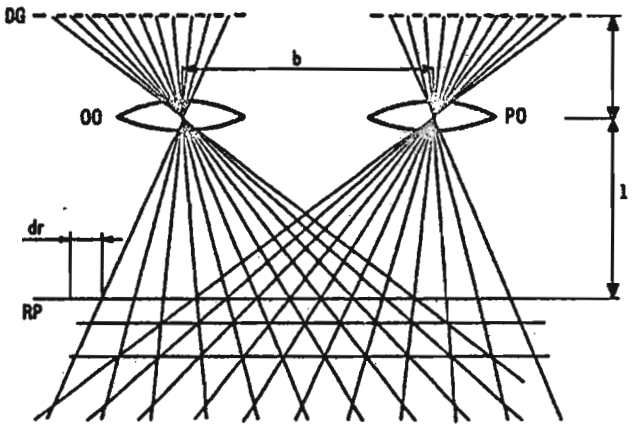

Fig. 4. Schematic representation of the projection moire topography which provides plane surface contours. PG – projection grating; PO – projection optics; OO – observation optics; DG – detection grating; RP – reference plane. For simplicity the objectives PO and OO are assumed to be thin lenses

The objective PO projects the periodic structure PG (amplitude diffraction grating) onto the surface under test. The image lines are no longer straight and equidistant when the object surface is not plane. The observation system OO images the object surface together with the projected structure onto the second periodic structure, called the detection/reference grating DG. Beating occurs between the spatial frequencies of the two structures resulting in the formation of moire fringes. Provided that certain geometrical conditions are fulfilled in the experimental system, the fringes follow the contours of the elevation of the object from the reference plane RP (coinciding with the image plane of PG).

The detailed studies of the geometrical conditions can be found, for example, in the papers of Pirodda (1969, 1982) and are summarized in the monograph by Patorski (1993). For the contouring surfaces to be plane (the most practical case) the following conditions must be fulfilled

- the entrance pupils of optical systems are equidistant from the reference plane (the line joining the centres of the entrance pupils of objectives PO and OO must be parallel to RP),
- the planes of gratings PG and DG are mutually parallel and parallel to RP,
- the lines of the gratings are set parallel (however, the shape of the contour surfaces does not depend on the direction of grating lines which need not be perpendicular to the join of PO and OO; the direction of lines influences the method sensitivity).

The distance of the Nth contouring plane from the reference plane is given by the following expression

$$z_N = \frac{Ndl(l-f)}{fb - Nd(l-f)} \tag{3.1}$$

where z_N is the distance of the Nth contouring plane from the reference plane, d is the period of projection and detection gratings, b is the separation distance between the optical axes, l is the distance from the join of entrance pupils to the reference plane, and f is the focal length of optical systems.

If the fringe interval Δz_N were constant, as in the case of collimated projection and telecentric observation, it would be equal to z_N/N. However Eq (3.1) applies to the general case of divergent beams (noncollimated projection allows contouring of large objects) and shows the fringe interval to increase with the distance to the reference plane. An approximation of Δz_N valid for practical cases can be derived by rewriting Eq (3.1) in the form

$$z_N = \frac{NldM_G}{b - NdM_G} = \frac{Nld_r}{b - Nd_r} \tag{3.2}$$

where M_G is the magnification of the projection, and d_r the period of the projected grating in the reference plane. Then

$$\Delta z = ld_r \frac{b}{b^2 - bd_r(2N+1) + d_rN(N+1)} = \frac{ld_r}{b - (2N+1)d_r} \tag{3.3}$$

if $b > d_r$. Ultimately when $b \gg Nd_r$, Δz is constant and

$$\Delta z = \frac{ld_r}{b} = d\frac{l}{b}\frac{l-f}{f} \tag{3.4}$$

The expression for resolution when projection and observation systems are telecentric is

$$\Delta \bar{z} = \frac{M_G d}{2\tan\alpha_0} \tag{3.5}$$

where α_0 is the angle between the normal to the reference plane and the direction of projection and observation. $\Delta \bar{z}$ is constant and independent of the distance between object and reference plane from the optics.

The resolution is increased (Δz decreased) by using a projected grating with small period d_r and by increasing the distance b between the optical axes (which in a telecentric system means increasing α_0). The latter is limited by the image quality of the projected grating, i.e., by the residual off-axis aberrations and vignetting in the projection optics. The latter can be counteracted by increasing the aperture, but it is at the cost of reducing the focal depth and then the height of profile which can be measured. The former can be counteracted by making

differential measurements using a specially prepared detection grating, Miles and Speight (1975).

On the other hand elimination of the factors mentioned above can be done at the stage of computer processing of the moire fringes. A reference surface is determined from the moire pattern obtained with the flat reference object. It is then subtracted from the final result when the object under test is being processed.

The configuration shown in Fig.4, using the detection grating in the image plane of observation optics, is the basic system for projection moire contouring of three-dimensional objects in real time. Real time relates here to the formation of moire fringes, without fringe pattern analysis.

There exist other real-time configurations with a single (projection and observation systems with axes intersecting) or double (optical axes of the two projectors can be parallel or symmetrically inclined and intersecting) projection systems. Because of the lack of space they will be not presented here. It can be said, however, that they are inferior to the configuration described above with respect to the simplicity of the opto-mechanical design, the contrast of moire fringes, the ease of interpretation of the results and the automation of the fringe pattern analysis process.

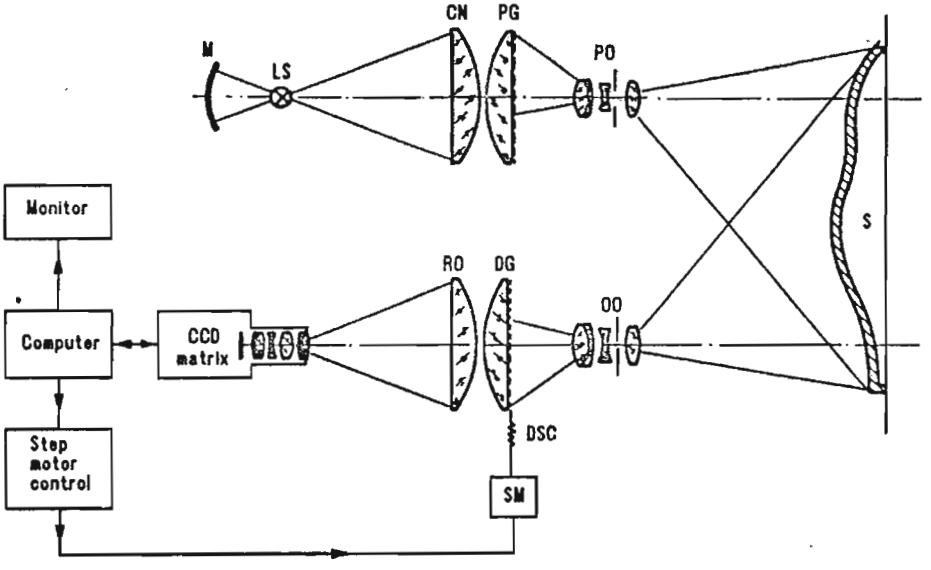

Fig. 5. Schematic representation of the projection moire equipment with a step-motor driven device for programmed displacement of the projection grating. LS – light source; M – mirror; CN – condenser; PG – projection grating; PO – projection objective; S – surface under test; OO – observation optics; DG – detection grating; RO – relay optics; SM – step motor; DSC – driving screw

Figure 5 shows the schematic diagram and a top-view of the projection moire

system designed and constructed at the Institute of Design of Precise and Optical Instruments of the Warsaw University of Technology. The apparatus uses the automatic fringe pattern analysis system implementing the temporal phase shifting method.

Although all versions of the phase shifting method (TPS, SPS, SCPS) may be used in moire topography and grating projection topography the temporal phase stepping is better suited for moire topography whereas the spatial carrier version seems an obvious choice for the grating projection technique.

The phase shifts δ_i required in the sequentially captured images are performed by the computer controlled stepping motor for lateral displacement of the projection grating.

The phase stepping method requires a sinusoidal profile of the fringes to be processed. Such a profile can be obtained readily by a slight defocusing the optical system which images theoretically triangular or trapezoidal profile fringes onto the photodetector. Usually three, four or five fringe pattern images are grabbed by a CCD camera and transferred to a computer memory. The images differ by a specified phase shift and the phase function at each pixel location is calculated according to the proper algorithm

- three-phase-step technique with $\delta_i = 2\pi/3$

$$\Phi(x,y) = \arctan\left[\sqrt{3}\frac{I_3(x,y) - I_2(x,y)}{2I_1(x,y) - I_2(x,y) - I_3(x,y)}\right] \tag{3.6}$$

where I_i are the intensity values in a single point of ith image.

This technique minimizes the acquisition time and the amount of memory required for storing data, but it is most sensitive to the phase shift and intensity errors;

- four-phase-step technique with $\delta_i = \pi/2$

$$\Phi(x,y) = \arctan\left[\frac{I_4(x,y) - I_2(x,y)}{I_1(x,y) - I_3(x,y)}\right] \tag{3.7}$$

This technique enables quick acquisition (still using one page frame grabber: 512 × 512 px.) with reduced sensitivity to the phase shift errors;

- five-phase-step technique with $\delta_i = \pi/2$

$$\Phi(x,y) = \arctan\left[\frac{2(I_2(x,y) - I_4(x,y))}{I_1(x,y) - 2I_3(x,y) + I_5(x,y)}\right] \tag{3.8}$$

This is the self-calibrating procedure for linear and big part of quadratic phase step errors. In general the highest accuracy is obtained when using this procedure. However the acquisition time increases and it may cause stronger influence of random environmental errors.

The decision to use the proper algorithm has to be taken on the base of given experimental setup, measurement requirements and the errors expected. The accuracies achieved in typical experimental arrangements are equal to $1/20 \div 1/40$ of the basic sensitivity (contour interval) of the particular configuration.

The phase calculated by one of the procedures, Eqs (3.6) $\div$ (3.8) is unwrapped, i.e., converted from the function $\Phi \bmod(2\pi)$ into a continuous function and then implemented into Eq (3.2) to calculate the properly scalled height distribution.

As mentioned above the achievable resolution can be varied by choosing the proper values of the parameters l, b, and d_r. However the design compromise between the contour interval Δz, the dimensions of the object under test and the depth of focus, respectively, should be reached. These are the basic functional parameters of the system. For example, for a typical projection distance $l = 3.5$ m, the base width $b = 350$ mm, the grating period $d = 0.1$ mm and the focal length $f = 210$ mm, the sensitivity expressed by the contouring interval Δz is 15.6 mm per fringe in the test field 1.1×1.1 m^2. With the help of the fringe pattern processing by the phase stepping method the sensitivity is 0.75 mm (Rafałowski, 1992).

The projection moire method has found the following exemplary applications
- measurement of strain in safety engineering
- selection of components produced by some technological processes
- automation of technological processes - "machine vision"
- vibration analysis
- human engineering.

Figure 6 shows an example of absolute contouring fringes on a welded brass element used for ship construction, the contour interval is 10 mm.

All versions of projection moire mentioned above have an actual grating in the observation system. Mostly the grating is made photographically. An alternative approach is to use a spatially modulated photodetector instead of the grating. For example, the spatial periodicity of the CCD photomatrix can be exploited (Nordbryhn, 1983). If a periodic or quasiperiodic input pattern is focused on such a periodic detector whose elements are sequentially sampled, and if the period of the pattern is close to the sampling period, a low frequency moire signal is obtained. This signal occurs when a quasi-periodic image contains certain low frequency components which are brought out as an alias due to undersampling. A sampling theorem for moire contouring was formulated by Bell and Koliopoulos (1981). Figure 7 shows the experimental results obtained using this technique.

The apparatus using the CCD photomatrix as the detection grating was designed (Rafałowski, 1992) to study the objects of dimensions up to 150×150 mm^2 with minimized projection distance. For $l = 700$ mm, $b = 180$ mm the basic contour interval is 2 mm per fringe, and the sensitivity after applying the phase stepping algorithm is 0.1 mm.

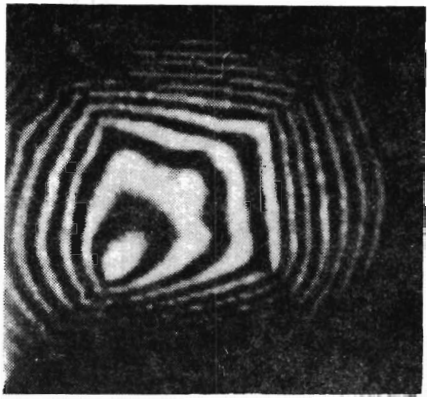

Fig. 6. Contour map of a welded brass element

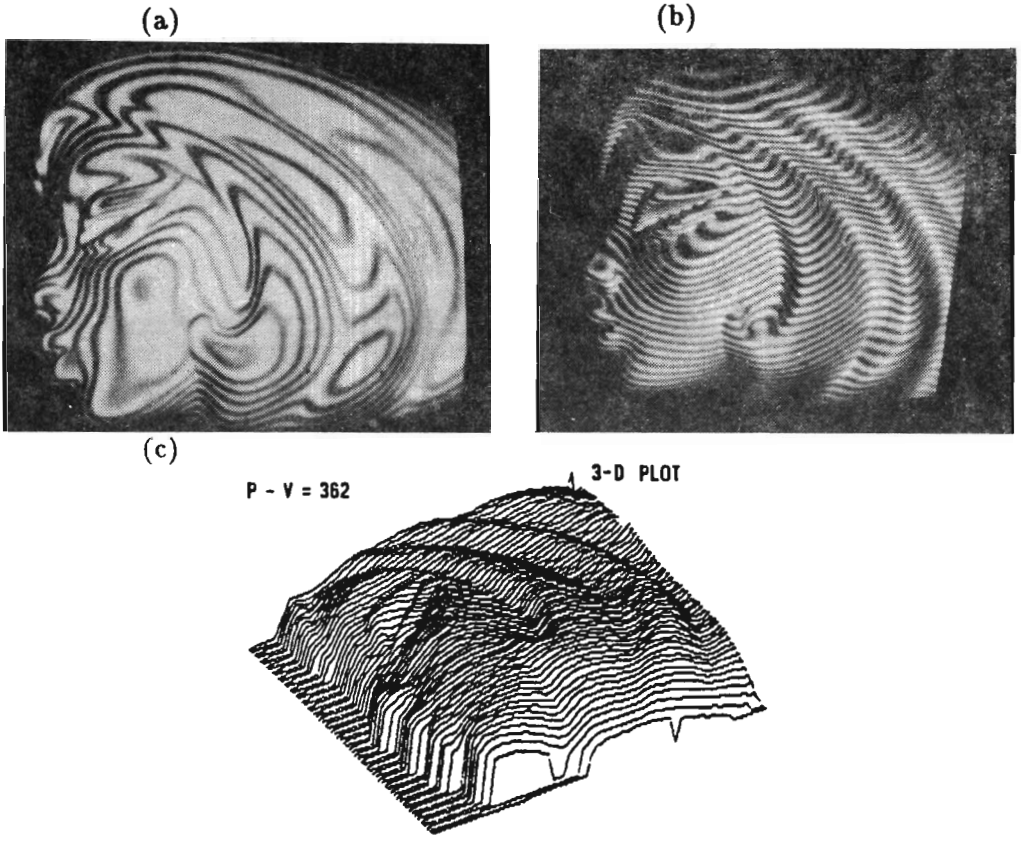

Fig. 7. Moire topography map obtained using the CCD photomatrix as the detection grating; (a) uniform field detection mode (the lines of the projection and detection grating are mutually parallel); (b) finite fringe detection mode (lines mutually inclined); (c) calculated three-dimensional map of the object under test

The two moire systems developed cover the range of scientific and technical applications for the 3-D object shape and deformation measurement with the sensitivity of a few tenths of mm and lower. If higher sensitivity is required the grating/fringe pattern projection topography (see Section 4 below) or interferometric methods (see Part II of this paper) should be applied.

4. Grating/fringe projection topography

An alternative approach to moire is the analysis of the deformed periodic structure itself without using a detection reference. Two basic arrangements of the projection system can be adopted

1. The optics projects, under incoherent illumination, the most commonly available Ronchi (square wave transmission) type grating or specially prepared sinusoidal grating slide. As mentioned above, sinusoidal intensity distribution is required for the phase stepping algorithm. Since accurate sinusoidal grating manufacturing is quite cumbersome, the use of a defocused image of projected square-wave Ronchi grating is preferred. The analysis of phase-stepping profilometry using defocused Ronchi grating projection can be found in the papers by Halioua and Liu (1986) and Su et al. (1992). It is worthwhile to mention that binary gratings can be conveniently programmed and displayed by a liquid crystal display (LCD) what opens the possibility for development of all-electronic LCD grating projection topography.

2. A sinusoidal intensity distribution on the object under test is generated by two beam interference (Srinivasan et al., 1983; Halioua and Liu, 1989). To minimize the influence of the environment (vibrations, turbulences) on the stability of an interferogram compact common path interferometers should be used. The lateral shearing interferometers using polarization elements are recommended in such a case.

The optical configurations used for the grating projection topography with incoherent illumination can have the geometries with parallel (Takeda and Mutoh, 1983; Su et al., 1988) and intersecting (Halioua and Liu, 1986; Su et al., 1992; Srinivasan et al. 1983, Halioua and Liu, 1989; Pirga and Kujawińska, 1993) optical axes of the projection and observation systems. In both cases to have the possibility of measuring large objects the diverging illumination is used. Such geometries result in curved and unequally distributed contours which might cause significant errors in shape determination. The most useful configuration is shown schematically in Fig.8.

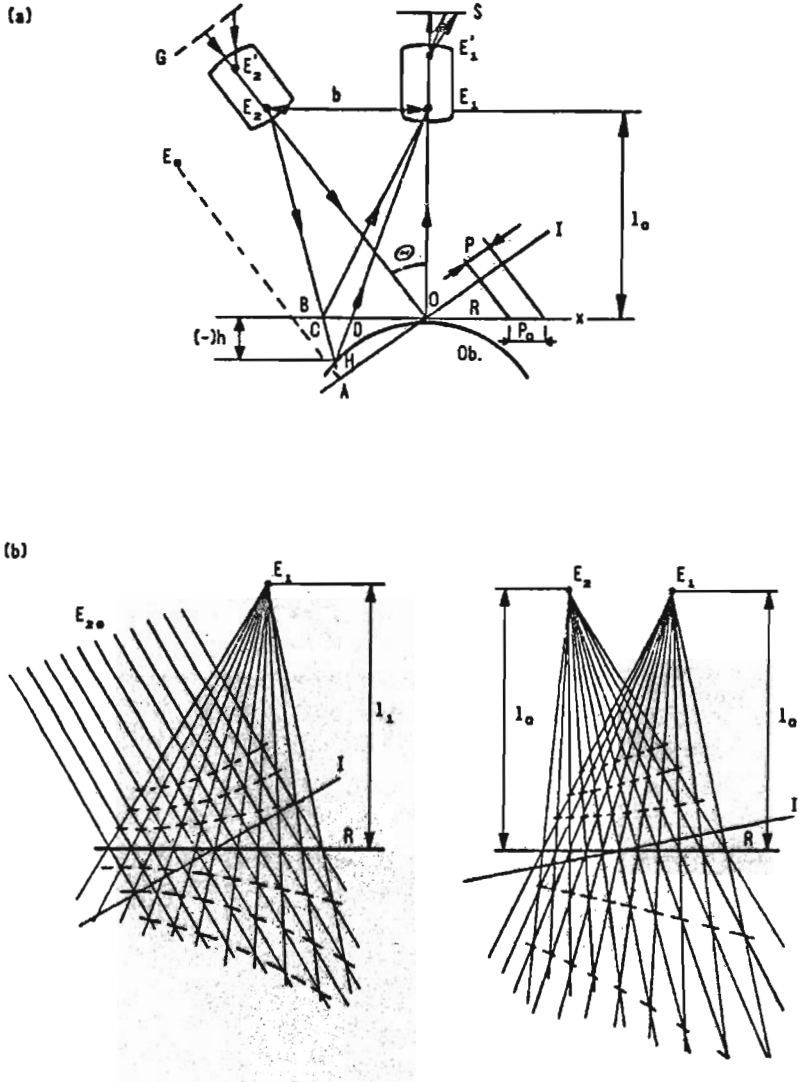

Fig. 8. General configuration of the grating projection topography with the intersecting axes of the projection and detection optics; (a) optical geometry; (b) schematic representation of contouring surfaces

The optical axis E_2E_2' of the projection optics intersects the axis E_1E_1' of the observation optics at point O on the reference plane. E_1, E_1' and E_2, E_2' denote the centres of the entrance and exit pupils of the projection and camera objectives, respectively. Grating G has its lines perpendicular to the figure plane and its image is formed on plane I. The object height is measured from the fictious reference plane R. For an arbitrary object the deformed periodic structure is given by

$$I(x,y) = a(x,y) + b(x,y)\cos[2\pi f_0 x + \Phi(x,y)] \tag{4.1}$$

where

$$\Phi(x,y) = 2\pi f_0 BD = 2\pi f_0(BC + CD) = \Phi_0(x,y) + \Delta\Phi(x,y)$$

$a(x,y)$ – background intensity,

$b(x,y)$ – fringe intensity amplitude,

f_0 – spatial frequency of the grating image.

Phase $\Phi(x,y)$ to be determined consists of two terms, where $\Delta\Phi(x,y)$ is the direct measure of the object height and $\Phi_0(x,y)$ relates to the deformation of the projected grating lines in case when the plane serves as the object. The latter term introduces a systematic error to the object height, where the latter one is given by

$$h(x,y) = \frac{l_0\Phi(x,y)}{\Phi(x,y) - 2\pi f_0 b} \tag{4.2}$$

To eliminate the error caused by $\Phi_0(x,y)$ two procedures can be used

1. Setup calibration

   A real flat object is placed in the reference plane R and the phase Φ_0 in the fringe pattern describes the systematic error related to the uneven contour plane distribution. This phase value is determined by the temporal or spatial carrier phase shifting method. It is then subtracted from the phase $\Phi(x,y)$ obtained in the same arrangement for the object under test. The calibration of the system has to be conducted after each change in the system geometry since the error varies with l and b. It is worthwhile mentioning that this procedure eliminates also the systematic errors caused by the aberrations and misalignments of the optical system.

2. Theoretical correction

   The second approach capitalizes upon the subtraction of theoretically determined value $\Phi_0(x,y)$ from the value $\Phi(x,y)$ obtained from the measurement. The phase $\Phi_0(x,y)$ is determined by the length BC, Fig.9, i.e.

$$BC = \frac{x^2 b}{l^2 + b^2 + |x|b} \tag{4.3}$$

The phase correction is $\Phi_0(x,y) = 2\pi f_0 BC$. Although this approach enables automatic correction for arbitrary values of l and b, it does not include the influence of aberration and misalignment errors.

The phase distributions $\Phi_0(x,y)$ or $\Phi(x,y)$ are determined by the phase shifting method. The principle of the temporal approach has been explained in Section 3, it is the same for the grating projection topography with an additional operation to be performed, namely: the subtraction of a linear carrier corresponding to the surface tilt.

However for the measuring method under consideration the carrier frequency phase shifting method seems to be an obvious choice. In short, its main requirement is to introduce a proper carrier frequency f_0 into the analyzed fringe pattern, i.e., f_0 is four times lower than the sampling frequency of the detector (one average fringe period should cover 4 camera pixels). It introduces a known constant phase shift between successive pixels, Eq (2.4). If the following basic assumptions are fulfilled (Kujawińska and Wójciak, 1991)

– the carrier frequency such that the phase in the sequential pixels differs by $\pi/2$

– the sinusoidal profile of the analysed fringes

– slowly varying background and contrast functions,

the phase in the sequential pixels can be calculated according to the standard five-phase-shift algorithm (Eq (3.8), where I_i is the intensity in the sequential pixels, i.e., $I_1(i-2,j),...,I_5(i+2,j)$ and (i,j) is the co-ordinate (x,y) given in number of pixels. After calculating the phase $\Phi'(x,y)$, the tilt previously introduced by the carrier frequency has to be removed by

$$\Phi'(i,j) = \Phi(x,y) - i\frac{\pi}{2} \tag{4.4}$$

Then the unwrapping procedure and the proper scaling are used to obtain the continuous shape map.

Figure 9 shows exemplary experimental results of measuring the microprofile of the surface of glass fibre/epoxy composite after the impact introduced by a steel ball (Pirga, Jancelewicz and Kujawińska, 1993). The peak-to-valley value of the measured shape was approx. 150μm and the shape was detected with the accuracy $\pm 1\mu$m.

As mentioned above, besides using a defocused image of binary amplitude grating the two beam interference can be employed to project a periodic structure on the object under test. Figure 10 shows an exemplary solution to this problem (Halioua and Liu, 1989).

Linearly polarized laser beam is spatially filtered by microscope objective with a pinhole and subsequently sheared by a Wollaston prism W. The phase modulator consists of a quarter-wave plate Q and a rotable polarizer P. By rotating

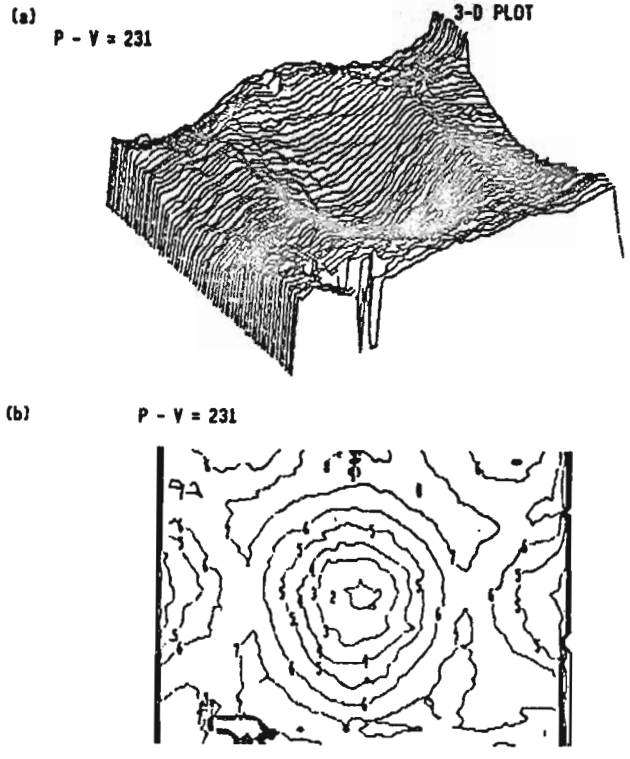

Fig. 9. Experimental results of measuring the surface shape of a glass fibre/epoxy composite after a steel ball impact; (a) 3-D plot; (b) contour map of the surface shape

the polarizer the sinusoidal intensity distribution of the interference pattern is translated laterally. A 180° rotation of the polarizer corresponds to a 2π phase modulation, and this permits very precise phase shifts. With the Wollaston prism located in the converging or diverging beam the fringe period can also be easily changed by an axial translation of the prism. Care must be taken, however, when generating high fringe density patterns where optical aberrations might cause the nonuniformity of the fringe period over the required field of view.

In Fig.10 the telecentric imaging configuration (objectives L_3 and L_4 with the focal plane stop) together with the plane wavefront illuminating beam is presented. In such a configuration the fringe intervals are constant with depth. The sensitivity Δz is given by

$$\Delta z_t = \frac{d_r}{\tan\alpha} = \frac{d}{\sin\alpha} \tag{4.5}$$

where d is the fringe period in the object space measured in the plane perpendicular to the axis of the projection system, d_r is the fringe period in the reference

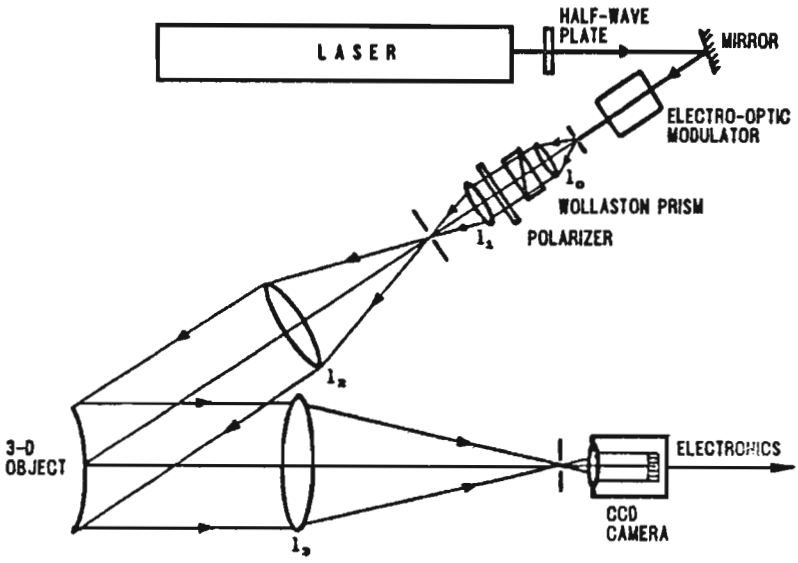

Fig. 10. Sinusoidal intensity distribution projection system with the phase shifter for the phase-stepping algorithm implementation (Halioua and Liu, 1989)

plane (perpendicular to the axis of the observation/detection system) and α is the angle between the axes of the two systems, see Fig.10.

The reported accuracy obtained by the interference fringe projection method depends on the surface finish of the object under test and the magnitude of the errors influencing the phase-stepping algorithm. It can vary from a few microns to tenths of a millimeter over the field of view of a few centimeters in diameter.

5. Conclusions

Means of automated data reduction have made possible for the optical testing methods to progress from the specialised photomechanics laboratory into a broader range of tests and research fields. The variety of computer fringe pattern processing methods, especially the so-called phase measuring methods, when implemented in the user friendly expert systems, enable fast analysis and interpretation of the experimental results even by the persons not specialising in optics.

The comparison of the phase measuring methods developed and applied to the expert fringe analysis system was presented. The advantages of the methods were clearly proved in the modern topography techniques using moire or grating projection approaches. In these techniques the phase-stepping algorithm can be

readily applied resulting in achieving much higher accuracies and a considerable time reduction when compared with the conventional methods of the shape and out-of-plane displacement topography.

In the second part of the work the developments in the automation of the data reduction process in high sensitivity grating interferometry used for submicron in-plane displacement studies will be presented.

References

1. AUGUSTYN W.H., 1979, *Automatic data reduction for both simple and complex interference patterns*, Proc. SPIE **171**, 22-31
2. BELL B.W., KOLIOPOULOS CH.L., 1984, *Moire topography, sampling theory, and charged-coupled devices*, Opt. Lett., **9**, 171-173
3. CHIANG F.P., 1979, *Moire methods of strain analysis*, Exp. Mech., **19**, 290-308
4. CREATH K., 1988, *Phase-measurement interferometry techniques*, Progress in Optics, ed.E.Wolf, **26**, 350-393
5. DURELLI A.J., PARKS V.J., 1970, *Moire Analysis of Strain*, Prentice Hall, Englewood Cliffs
6. DYSON J., 1963, *The rapid measurement of photographic records of interference fringes*, Appl. Opt., **2**, 487-489
7. HALIOUA M., LIU H.C., 1986, *Optical sensing techniques for 3-D machine vision*, Proc. SPIE, **665**, 150-161
8. HALIOUA M., LIU H.C., 1989, *Optical three-dimensional sensing by phase measuring profilometry*, Opt. Lasers Eng., **11**, 185-215
9. JONES R.A., KADAKIA P.L., 1968, *An automated interferogram analysis*, Appl. Opt., **7**, 1477-1481
10. KUJAWIŃSKA M., WÓJCIAK J., 1991, *Spatial phase-shifting techniques of fringe pattern analysis in photomechanic*, Proc. SPIE **1554B**, 503-513
11. KUJAWIŃSKA M., WÓJCIAK J., 1991a, *High accuracy Fourier transform fringe pattern analysis*, Opt. Lasers in Eng., **14**, 325-339
12. MILES C.A., SPEIGHT B.S., 1975, *Recording the shape of animals by a moire method*, J. Phys.E., **8**, 773-776
13. NORDBRYHN A., 1983, *Moire topography using a charge coupled device television camera*, Proc. SPIE, **398**, 208-213
14. PATORSKI K., 1993, *Handbook of the Moire Fringe Technique*, Elesevier Science Publishers, Amsterdam
15. PIRGA M., JANCELEWICZ B., KUJAWIŃSKA M., FILIPOWSKI R., 1993, *Fringe projection technique for measurement of a local damage trace on the surface of multilayer composite structures*, J.Theor.Exp.Mech., submitted for publication
16. PIRGA M., KUJAWIŃSKA M., 1993, *Modified procedure for automatic surface topography* , Measurement, in press

17. PIRODDA L., 1969, *Principi e applicazioni di un metodo fotogrammetrico basato sull impiego del moire*, Rivista di Ing., 12, 913-923

18. PIRODDA L., 1982, *Shadow and projection moire techniques for absolute or relative mapping of surface shapes*, Opt. Eng., 21, 640-649

19. RAFAŁOWSKI M., 1992, *Zautomatyzowane urządzenia do bezkontaktowych pomiarów kształtu i deformacji metodą mory projekcyjnej*, Pom.Aut.Kontr., 240-242

20. SCHWIDER J., 1990, *Advanced evaluation techniques in interferometry*, Progress in Optics, 28, 271-359

21. SCIAMMARELLA C.A., 1982, *The moire method-a review*, Exp.Mech., 22, 418-433

22. SRINIVASAN V., LIU H.C., HALIOUA M., 1984, *Automated phase-measuring profilometry of 3-D diffuse objects*, Appl.Opt., 23, 3105-3108

23. SU X.Y., LI J., GUO R.R., SU W.Y., 1988, *An improved Fourier transform profilometry*, Proc. SPIE, 954, 241-244

24. SU X.Y., ZHOU W.S., VON BALLY G., VUKICEVIC D., 1992, *Automated phase-measuring profilometry using defocused projection of a Ronchi grating*, Opt. Commun., 94, 561-573

25. TAKEDA M.,1990, *Spatial-carrier fringe pattern analysis and it applications to interferometry and profilometry: An overview*, Industrial Metrology, 1, 79-99

26. TAKEDA M., MUTOH K., 1983, *Fourier transform profilometry for the automatic measurement of 3-D object shapes*, Appl.Opt., 22, 3977-3982

27. THEOCARIS P.S., 1969, *Moire Fringes in Strain Analysis*, Pergamon Press, Oxford

Nowe kierunki rozwoju optycznych metod mechaniki doświadczalnej. Część I: Metody mory i projekcji rastra do pomiaru kształtu i deformacji

Streszczenie

Scharakteryzowano wpływ dynamicznego rozwoju komputerów osobistych i technik video na optyczne metody badań w mechanice doświadczalnej. Przedstawiono nowe metody komputerowego przetwarzania informacji zawartej w interferogramach/moiregramach ze szczególnym uwzględnieniem tak zwanych metod fazowych. Podkreślono zalety różnych wersji metody dyskretnej zmiany fazy i zilustrowano je przykładowymi wynikami prac eksperymentalnych z zakresu topograficznych metod mory i projekcji rastra. Praca zawiera również opis opracowanej aparatury i dyskusję dokładności metod. Badanie przemieszczeń w płaszczyźnie metodą interferometrii siatkowej będzie przedmiotem drugiej części pracy.

Manuscript received March 18, 1993; accepted for print March 31, 1993